A multicommodity kinematic wave simulation model of network traffic flow

November 12, 2003

W.L. Jin[1]

Department of Mathematics

University of California

Davis, CA 95616

Tel: 530-752-0828

Fax: 530-752-6635

E-mail: wjin@ucdavis.edu

H.M. Zhang[2]

Department of Civil and Environmental Engineering

University of California

Davis, CA 95616

Tel: 530-754-9203

Fax: 530-752-7872

E-mail: hmzhang@ucdavis.edu

Word Count: 7500 (approximately)

ABSTRACT

In this paper, we propose a multi-commodity, discrete kinematic wave model for simulating network traffic flow that possesses the theoretical rigor and computational efficiency inherent in the kinematic wave theory. In this model,

[1]Author for correspondence (Current address: Institute of Transportation Studies / University of California / 522 Social Science Tower / Irvine, CA 92697-3600 / (949) 824-2949 / (949) 824-8385 Fax / wjin@uci.edu)

[2]CKS Professor, School of Transportation Engineering, Tongji University, Shanghai, China.

fluxes through boundaries and junctions are computed systematically under the supply-demand framework. In addition, traffic is also modelled by commodity type such that the effects of the geometrical characteristics of a road network on traffic dynamics can be captured. Although traffic is not ordered down to the vehicle level as in existing kinematic wave simulation models, the non-compliance to First-In-First-Out in this model is still in the order of Δt, the time increment. Hence travel times in the average sense can be defined from cumulative curves. Finally, the evolution of traffic dynamics in a sample road network is shown to demonstrate the stability, numerical convergence and soundness of the proposed network kinematic wave model.

1 Introduction

Recurrent or non-recurrent traffic congestion in many major metropolitan areas have seriously deteriorated the mobility of people and goods. To tackle the congestion problem, traffic engineers and scientists are facing a number of challenges. These include the evaluation of transportation network performance, prevention and efficient management of incidents, development of effective traffic control strategies, and the estimation of traffic demand, to mention a few. As we know, a fundamental issue in addressing all these challenges is the understanding of traffic dynamics on a road network, i.e., the evolution of traffic on a road network under initial and boundary conditions, for which traffic flow models of road networks play an important role.

Among many traffic flow models, the kinematic wave models offer many advantages in studying traffic dynamics in large-scale road networks. Practically, people are more interested in aggregate-level traffic conditions such as average travel speeds, densities, flow-rates, and travel times, which are directly concerned or can be easily derived in the kinematic wave models. Theoretically, the evolution of traffic conditions on a link can be studied as hyperbolic conservation laws, which provides rigor to the analysis. Computationally, the kinematic wave models can be solved efficiently with the Godunov method (1, 2), which offers computational efficiency in large-scale applications.

There are several approaches in modelling network traffic flow under the framework of kinematic wave theory. First, Vaughan et al. (3) studied network traffic flow with two continuous equations: a "local equation", which ensures traffic conservation and is consistent with the traditional LWR model on a link at the aggregate level, and a "history equation", which computes the trajectory of each vehicle at the disaggregate level. Since the trajectories of all vehicles are not always required for many applications, this model consumes significant amount of computational resources than necessary. Second, Jayakrishnan (4) introduced a discrete network flow model, in which each link is partitioned into a number of cells, vehicles adjacent to each other and with the same O/D and path are called a "macroparticle", and the position of a macroparticle at each time step is determined by its travel speed and the cell's length. However, with the given mechanism, this model may not be consistent with the LWR model since traffic conservation can be violated. Third, Daganzo (1) introduced a network flow model based on his Cell Transmission Model (CTM) (5), a numerical approximation of the LWR model with a special fundamental diagram — a triangle. In this discrete model, macroparticles in the sense of Jayakrishnan (4) in a cell are ordered according to their waiting times and moved to the downstream cell when their waiting times are greater than a threshold minimum waiting time, which is computed from traffic flow at the aggregate level. However, the determination of the threshold minimum waiting time is quite tedious. Fourth, in the KWave98 simulation package (6), which is based on the simplified kinematic wave theory by Newell (7), vehicles on a link are considered to be ordered as a queue. Then, with the in-queue and out-queue of the link determined, one can easily update the link queue. However, in-queues and out-queues at typical highway junctions such as merges and diverges create difficulties for this model.

In many applications, such as dynamic traffic assignment (DTA), the First-In-First-Out (FIFO) property is a key concern. Consequently, all the aforementioned models order vehicles albeit in different fashions. Vehicles are ordered according to their trajectories in (3), locations in (4), waiting times in (1), and positions in a link queue in (6). That is, these simulation models track either vehicles' trajectories, or positions, or waiting times, or queuing orders. [3] In these models, therefore, traffic conditions are also considered at the vehicle level. As a result, the computational efficiency of the kinematic wave models is not fully utilized.

In contrast, (8, 9) proposed the so-called STRADA model. In this model, the Godunov-type approximation is applied, traffic flows through network junctions as well as link boundaries are computed in the framework of supply-demand method (2), and traffic is disaggregated into partial traffic according to destinations, origin-destination pairs, paths, etc. Further, dynamics of partial flows are computed based on the theory in (2). Since this model does not consider individual vehicles, computational cost does not increase with the number of vehicles as in the aforementioned models. Thus it is more efficient in simulating large networks. However, since vehicles are not ordered explicitly in this model, the FIFO rule is not exactly followed even on a link or path.

In the same spirit as in (8, 9), we propose in this paper a new discrete network traffic flow model for a simple traffic system, where vehicles are categorized into multiple commodities according to their paths and no differentiations are made in vehicle types, driver classes, or lane types (such as HOV lanes). We hereafter refer to this model as multi-commodity, discrete kinematic wave (MCDKW) model. In the MCDKW model, besides link characteristics such as free flow speed, capacity, and number of lanes, traffic dynamics are highly

[3] In (4), although the introduction of macroparticles save a certain amount of memory in computation, this saving is diminished when vehicles of different classes are evenly mixed.

related to geometrical characteristics of a road network including link inhomogeneities, merges, diverges, and other junctions. Although it does not give a complete, detailed picture of traffic dynamics as a microscopic traffic simulation model does, this model is still of importance for many applications, in which the difference in vehicles, drivers, or lanes are negligible or can be averaged out without major loss of accuracy.

Like in the STRADA model, the complexity of computation in the MCDKW model is not related to the number of vehicles. However, although having the same framework as the STRADA model, the MCDKW model is different from the former in the following aspects. First, in the MCDKW model, we specify commodity flows as path flows. Therefore, FIFO is satisfied for each commodity as long as it is satisfied for each link. Further, user equilibrium is not needed in order to define experienced commodity travel times. While in the STRADA model, instantaneous travel time is used. In this sense, although the MCDKW is not so flexible as the STRADA model, it can be used as a rigorous analysis tool for network traffic dynamics without considering user equilibrium and for traffic assignment methods based on experienced travel time. Second, the MCDKW model, we incorporated our latest efforts in improving kinematic wave models for highway junctions. In the STRADA model, intersection zones are defined to incorporate junction models. In stead, we applied a simpler merge model and a simpler diverge model, which in turn lead to a simpler model for general junctions. As a result, complex junctions can be treated as simple junctions without decomposing them into simpler ones, and separate treatment on intersections is not needed. Further, in these models, we do not need any parameters other than those contained in the fundamental diagram. Because of the differences, the MCDKW model is computationally more efficient and can be calibrated more easily. Third, based on commodity travel times, we can show that the MCDKW model is convergent by numerical simulations. This directly addresses the FIFO concerns in such macroscopic models.

In the rest of this paper, we will discuss theories underlying the MCDKW model in Section 2. In Section 3, we will discuss the process of output from the MCDKW model to obtain interested data of a road network, such as travel times. In Section 4, we carry out some numerical simulations of a simple road network. In Section 5, we will draw some conclusions and provide further discussions about the calibration of the MCDKW model.

2 Underlying theories of the MCDKW model

In the multi-commodity discrete kinematic wave (MCDKW) network traffic flow model, dynamics of total traffic, i.e., the evolution of traffic conditions of all commodities, are studied at the aggregate level and governed by the kinematic wave theories. These theories provide the building blocks for the MCDKW model. At the disaggregate level, traffic of each commodity in the form of proportions is studied with its proportion, and First-In-First-Out property on a link will be discussed.

2.1 Kinematic wave theories at the aggregate level

In the MCDKW model, we use the discrete form of the kinematic wave theories, which can be obtained through the first-order[4] Godunov method (11) of the continuous versions. In the discrete form, each link is partitioned into N cells, of equal length or not, and the time interval is discretized into K time steps. Then, we obtain the Godunov-type finite difference equation for total flow in cell i from time step j to time step $j+1$ as follows:

$$\frac{\rho_i^{j+1}-\rho_i^j}{\Delta t}+\frac{f_{i-1/2}^{j*}-f_{i+1/2}^{j*}}{\Delta x} = 0, \tag{1}$$

where Δx is the length of cell i, Δt is the time from time step j to time step $j+1$, and the choice of $\frac{\Delta t}{\Delta x}$ is governed by the CFL (12) condition. In Equation

[4] A second-order method was discussed in (10).

1, ρ_i^j is the average of traffic density ρ in cell i at time step j, similarly ρ_i^{j+1} is the average of ρ at time step $j+1$; $f_{i-1/2}^{j*}$ is the flux through the upstream boundary of cell i from time step j to time step $j+1$, and similarly $f_{i+1/2}^{j*}$ is the downstream boundary flux. Fluxes through link boundaries, merges, diverges, or general junctions are discussed later in details. Given traffic conditions at time step j, we can calculate the traffic density in cell i at time step $j+1$ as

$$\rho_i^{j+1} \quad = \quad \rho_i^j + \frac{\Delta t}{\Delta x}(f_{i-1/2}^{j*} - f_{i+1/2}^{j*}). \tag{2}$$

Defining $\mathbf{N}_i^j = \rho_i^j \Delta x$ as the number of vehicles in cell i at time step j, $\mathbf{N}_i^{j+1} = \rho_i^{j+1}\Delta x$ as the number of vehicles at time step $j+1$, $F_{i-1/2}^j = f(\rho_{i-1/2}^{j*})\Delta t$ as the number of vehicles flowing into cell i from time step j to $j+1$, and $F_{i+1/2}^j$ as the number of vehicles flowing out of cell i, Equation 2 can be written as:

$$\mathbf{N}_i^{j+1} \quad = \quad \mathbf{N}_i^j + F_{i-1/2}^j - F_{i+1/2}^j, \tag{3}$$

which is in the form of traffic conservation.

Given the initial and boundary conditions, we will use the supply-demand method (1, 2) for computing fluxes through cell boundaries: $F_{i-1/2}^j$ or $f_{i-1/2}^{j*}$. In a general road network, there are the following types of boundaries: boundaries inside a link, merges, diverges, and more complicated intersections.

1. When the boundary at $x_{i-1/2}$ is a boundary inside a link, whose upstream cell is denoted as u and downstream cell d, we follow the supply-demand method discussed in (1, 2, 13). I.e., if we define the upstream demand as

$$D_u \quad = \quad \begin{cases} Q(U_u), & \text{when } U_u \text{ is under-critical (UC)} \\ Q_u^{max}, & \text{when } U_u \text{ is over-critical (OC)} \end{cases} \tag{4}$$

and define the downstream supply as

$$S_d \quad = \quad \begin{cases} Q_d^{max}, & \text{when } U_d \text{ is under-critical} \\ Q(U_d), & \text{when } U_d \text{ is over-critical} \end{cases} \tag{5}$$

then the boundary flux can be simply computed as

$$f^{j*}_{i-1/2} = \min\{D_u, S_d\}, \tag{6}$$

where U_d and U_u are traffic conditions including density ρ and road inhomogeneity a at jth time step, of the downstream and upstream cells, respectively. As discussed in (13), this method is consistent with analytical solutions of the Riemann problem for inhomogeneous roadway.

2. When $x_{i-1/2}$ is a merging junction with P upstream merging cells, which are denoted as u_p $(p = 1, \cdots, P)$, and a downstream cell d. The demand of upstream cell u_p, D_p, is defined in Equation 4, and the supply of the downstream cell, S_d, is defined in Equation 5. Then, we apply the simplest distribution scheme (14) and compute the boundary fluxes as

$$\begin{aligned} f^{j*}_{i-1/2,d} &= \min\{\textstyle\sum_{p=1}^{P} D_p, S_d\}, \\ f^{j*}_{i-1/2,u_p} &= f^{j*}_{i-1/2,d}\frac{D_p}{\sum_{p=1}^{P} D_p}, \quad p = 1, \cdots, P, \end{aligned} \tag{7}$$

where $f^{j*}_{i-1/2,d}$ is the in-flow of the downstream cell, and $f^{j*}_{i-1/2,u_p}$ is the out-flow of upstream cell u_p.

In addition, if an upstream cell, e.g. u_p, is signalized and denote r as the proportion of green light in a cycle (i.e. green ratio), then we can apply the controlled traffic demand of u_p, $\min\{rQ^{max}_p, D_p\}$, in the supply-demand method above (1, 14). Note that r can be a continuous function when considering the average effect or a piece-wise constant function when the simulation interval Δt is smaller than a signal cycle.

3. When $x_{i-1/2}$ is a diverging junction with P downstream cells, which are denoted as d_p $(p = 1, \cdots, P)$, and an upstream cell u. In the model proposed in (15), we introduced a new definition of partial traffic demand of vehicles travelling to d_p in cell u as follows,

$$D_p = \begin{cases} Q(\rho_p; \hat{\rho}_p) \equiv \rho_p\, V(\rho_p + \hat{\rho}_p) & \rho_p \text{ is UC} \\ Q^{\max}(\hat{\rho}_p) & \text{otherwise} \end{cases}, \tag{8}$$

where $\hat{\rho}_p$ is equal to the density of vehicles not travelling to d_p, and at critical density $Q(\rho; \hat{\rho}_p)$ reaches its maximum. The traffic supply for d_p, S_p, is defined by Equation 5. Then, the boundary flux to d_p, $f^{j*}_{i-1/2,d_p}$, can be computed by

$$f^{j*}_{i-1/2,d_p} = \min\{S_p, D_p\}, \tag{9}$$

and the out-flow of u, $f^{j*}_{i-1/2,u}$, is the sum of these flows,

$$f^{j*}_{i-1/2,u} = \sum_{p=1}^{P} f^{j*}_{i-1/2,d_p}. \tag{10}$$

Another model of traffic diverging to D downstream links we will implement in the MCDKW model was proposed in (1, 2):

$$\begin{aligned} f^{j*}_{i-1/2,u} &= \min_{d=1}^{D}\{D_u, S_d/\xi_d\}, \\ f^{j*}_{i-1/2,d} &= \xi_d f^{j*}_{i-1/2,u}, \qquad d = 1, \cdots, D, \end{aligned} \tag{11}$$

where ξ_d is the proportion of commodity d in total traffic, and here D_u is the demand of the upstream cell as defined in Equation 4.

When vehicles have no predefined route and can choose any downstream link at a diverge, we use the model proposed in (14):

$$\begin{aligned} f^{j*}_{i-1/2,u} &= \min\{D_u, \textstyle\sum_{d=1}^{D} S_d\}, \\ f^{j*}_{i-1/2,d} &= \frac{S_d}{\sum_{d=1}^{D} S_d} f^{j*}_{i-1/2,u}, \qquad d = 1, \cdots, D. \end{aligned} \tag{12}$$

4. For intersections with two or more upstream and downstream links, we can combine the merge and diverge models together. Note that only the computation of demands and supplies may change, and the supply-demand method is still the same.

   For example, when we combine the supply-demand methods in Equation 7 and Equation 11 for an intersection with U upstream branches and D

downstream branches, we can compute fluxes by

$$\begin{aligned}
f^{j*}_{i-1/2} &= \min_{d=1}^{D}\{\textstyle\sum_{u=1}^{U} D_u, S_d\Big/\left(\frac{\sum_{u=1}^{U} D_u \xi_{u,d}}{\sum_{u=1}^{U} D_u}\right)\},\\
f^{j*}_{i-1/2,d} &= \frac{\sum_{u=1}^{U} D_u \xi_{u,d}}{\sum_{u=1}^{U} D_u} f^{j*}_{i-1/2}, \qquad d = 1, \cdots, D, \\
f^{j*}_{i-1/2,u} &= \frac{D_u}{\sum_{u=1}^{U} D_u} f^{j*}_{i-1/2}, \qquad u = 1, \cdots, U,
\end{aligned} \tag{13}$$

where $\xi_{u,d}$ is the proportion of traffic heading downstream link d in upstream link u, $f^{j*}_{i-1/2}$ is the total flux through the boundary, $f^{j*}_{i-1/2,d}$ flux heading downstream link d, and $f^{j*}_{i-1/2,u}$ flux from upstream link u. In this model, the intersection is considered as a combination of a merge with U upstream branches and a diverge with D downstream links in the fashion of (1). Note that the merge model, Equation 7, and the diverge model, Equation 11, are specific cases of Equation 13.

2.2 Commodity-based kinematic wave theories

In the MCDKW model, commodities are differentiated by their origin-destination pairs or paths. We assume that a road network has P' origin-destination (OD) pairs and P paths ($P \geq P'$). When vehicles have predefined paths, we then have a P-commodity traffic flow on the road network and label vehicles taking pth path as p-commodity. When vehicles of an O/D have no predefined paths, we have P'-commodity traffic flow.

In the kinematic wave theories of multi-commodity traffic, we denote total traffic density, travel speed, and flow-rate respectively by ρ, v, and q, which are all functions of location x and time t. In contrast, these quantities for p-commodity vehicles are ρ_p, v_p, and q_p respectively. The fundamental diagram of total traffic defines a functional relationship between density and travel speed or flow-rate: $q = Q(a, \rho)$ and $v = V(a, \rho) \equiv Q(a, \rho)/\rho$, where $a(x)$ stands for road inhomogeneities at location x such as changes in the number of lanes, curvature, and free flow speed. Further, we assume traffic on all links is additive in the following sense (15):

$$\begin{aligned}
\rho &= \sum_{p=1}^{P} \rho_p, && (14)\\
v &= v_p = V(a,\rho), \qquad p = 1, \cdots, P, && (15)\\
q &= \sum_{p=1}^{P} q_p, && (16)
\end{aligned}$$

The kinematic wave theory of additive multi-commodity traffic on a link can be described by the following theory (13),

$$\begin{aligned}
\rho_t + Q(a,\rho)_x &= 0,\\
(\rho_p)_t + (\rho_p V(a,\rho))_x &= 0, \qquad p = 1, \cdots, P.
\end{aligned} \tag{17}$$

If denoting the local proportion of p-commodity $(p = 1, \cdots, P)$ by $\xi_p = \rho_p/\rho$, we then have the following advection equations (2)

$$(\xi_p)_t + V(a,\rho)(\xi_p)_x = 0, \qquad p = 1, \cdots, P. \tag{18}$$

From Equation 18, we can see that proportions of all commodities travel forward in a link along with vehicles in traffic flow, as the change of ξ_p in material space, $(\xi_p)_t + V(a,\rho)(\xi_p)_x$, equals to zero. This is also true for all kinds of junctions, in particular diverges, in their supply-demand models in the preceding subsection [5] Therefore, Equation 18 also means that the profile of proportions coincides with vehicles' trajectories on a link. That is, if two or more commodities initially completely are divided by an interface, this interface will move forward along with vehicles on its both sides, and these commodities will never mix. Since each single vehicle can considered as a commodity, all vehicles' trajectories keep disjoint in the commodity-based kinematic wave models. Therefore, FIFO principle is respected in this continuous model.

In the previous subsection, we studied the continuous kinematic wave theory for total traffic. Here, we will present the discrete kinematic wave theory for each commodity. Given traffic conditions of p-commodity at time step j, i.e.,

[5] That traffic is anisotropic is believed to regulate this property.

$\rho^j_{p,i}$ in all cells, we can calculate the traffic density of p-commodity in cell i at time step $j+1$ as

$$\rho^{j+1}_{p,i} \quad = \quad \rho^j_{p,i} + \frac{\Delta t}{\Delta x}(f^{j*}_{p,i-1/2} - f^{j*}_{p,i+1/2}), \tag{19}$$

where $f^{j*}_{p,i-1/2}$ is the in-flux of p-commodity through the upstream boundary of cell i during time steps j and $j+1$, and $f^{j*}_{p,i+1/2}$ out-flux. Furthermore, since the profile of the proportion of a commodity always travels forward at traffic speed, the proportion of a commodity in out-flux of cell i compared to all commodities is equal to the proportion of the commodity in the cell. I.e. (2),

$$f^{j*}_{p,i+1/2} \cdot \rho^j_i = f^{j*}_{i+1/2} \cdot \rho^j_{p,i}, \qquad p = 1, \cdots, P. \tag{20}$$

This is true for cells right upstream of merging junctions (14) and diverging junctions (16, 1, 2, 17).

During time steps j and $j+1$ at a boundary $x_{i+1/2}$, which has U upstream cells and D downstream cells, if we know the out-flux from upstream cell u ($u = 1, \cdots, U$), $f^{j*}_{p,u,i+1/2}$ ($p = 1, \cdots, P$), we can obtain the in-flux of downstream cell d ($d = 1, \cdots, D$), $f^{j*}_{p,d,i+1/2}$ ($p = 1, \cdots, D$), from traffic conservation in p-commodity:

$$\sum_{u=1}^{U} f^{j*}_{p,u,i+1/2} = \sum_{d=1}^{D} f^{j*}_{p,d,i+1/2}. \tag{21}$$

However, when p-commodity vehicles can take more than one downstream cells, we have

$$\sum_{p=1}^{P} f^{j*}_{p,d,i+1/2} = f^{j*}_{d,i+1/2}. \tag{22}$$

Note that, in Equation 17, the kinematic wave solutions are determined by those of total traffic, which are obtained by the first-order convergent Godunov method. Also from Equation 18, we can see that Equation 20 yields an up-wind method for ξ_p in Equation 19. Therefore, the discrete model for the commodity-based kinematic wave model, Equation 17, converges in first order to continuous version, whose solutions observe FIFO principle. That is, in numerical solutions, error in travel time of any vehicle is in the order of Δt. That is, in the MCDKW model, FIFO is accurate to the order of Δt and Δx. Therefore, when we decrease Δt, this approximation becomes more accurate.

3 Cumulative flow, travel time, and other properties of a road network

In the MCDKW simulation, we keep track of the change of traffic densities of all cells and fluxes through all boundaries. Besides, these quantities are specified for commodities. In this section, we will discuss how to obtain other traffic information from these quantities.

3.1 Cumulative flow and vehicle identity

Cumulative flow at a boundary $x_{i-1/2}$ from time t_0 to t, $N(x_{i-1/2};[t_0,t])$, is the total number of vehicles passing the spot during the time interval. If the flux is $f^*(x_{i-1/2},s)$ at time s, then we have

$$N(x_{i-1/2};[t_0,t]) \quad = \quad \int_{s=t_0}^{t} f^*(x_{i-1/2},s)\,\mathrm{ds}. \tag{23}$$

Correspondingly, the discrete cumulative flow, $N(x_{i-1/2};[J_0,J])$, which is from time steps J_0 to J, is defined as

$$N(x_{i-1/2};[J_0,J]) \quad = \quad \sum_{j=J_0}^{J-1} f_{i-1/2}^{j*}\,\Delta t, \tag{24}$$

where $f_{i-1/2}^{j*}$ is the flux at $x_{i-1/2}$ during time steps j and $j+1$.

A curve of cumulative flow versus time is also known as a Newell-curve or simply N-curve (5), since Newell (7) developed a simplified version of the LWR kinematic wave theory based on this concept.

From the definition of cumulative flow, we can see that an N-curve is non-decreasing in time. Further, it is increasing when passing flow is not zero.

Although densities and fluxes are quantities at the aggregate level, the MCDKW model is capable of tracking traffic information at the commodity level. This can be done also with cumulative flows: a vehicle passing a cell boundary at a time step can be labelled by the corresponding cumulative flow. If all cumulative flows are synchronized; for example, when the initial traffic in a road network is empty, then the same cumulative flow of a commodity refer to the same vehicle. This fact is due to the FIFO property in all commodities. [6]

Therefore, in the MCDKW simulation, with curves of cumulative flows as a bridge between the aggregate and disaggregate quantities, we are able to keep track of vehicle trajectories, accurate to the order of Δx and Δt, from cumulative flows at all cell boundaries. Further, with finer partition of each link, we can obtain more detailed information at the disaggregate level.

3.2 Travel time

In this subsection, we define commodity travel time, which is indeed path travel time, since a commodity consists of all vehicles using the same path. For a vehicle, which can be identified by its commodity cumulative flow number under FIFO, its travel time across a link or from the origin to the destination can be inferred from N-curves. For example, when we know its arrival and departure times to a link from the corresponding N-curves, we can easily compute its travel time across the link.

This can be demonstrated in Figure 2. In this figure, the left curve is the N-curve at location x_1, and the right curve at x_2. These two curves are synchronized in the sense that the vehicles between x_1 and x_2 at $t = 0$ are not counted in $N(x_2; [0, t])$. Therefore, from FIFO, we can see that the N_0 vehicle on the left N-curve is the same as the N_0 vehicle on the right N-curve. Then,

[6] When type 4 diverge appears, this has to be checked.

from the curve, we know that the times of the N_0 passing x_1 and x_2 are t_1 and t_2 respectively. Thus, its travel time from x_1 to x_2 is $t_2 - t_1$.

In Figure 2, the left N-curve reaches a maximum at some time and stop increasing after that. This means that no flow passes x_1 after that time. The right N-curve has the same pattern. In such cases, one has to be cautious when computing travel time for the last vehicle, identified by the maximum cumulative flow, which corresponds to multiple values in time. Rigorously, therefore, the time for a vehicle N_0 passing a location x, where the N-curve is $N(x;[t_0,t])$, can be defined by

$$T(N_0;x) \quad = \quad \min_s \{s \big| \text{when } N(x;[t_0,s]) = N_0\}. \tag{25}$$

Further, the travel time for the N_0 vehicle from x_1 to x_2 is

$$T(N_0;[x_1,x_2]) \quad = \quad T(N_0;x_2) - T(N_0;x_1). \tag{26}$$

With the definition of passing time in Equation 25, at x, the vehicle identity N_0 has a one-to-one relationship with its passing time $T(N_0;x)$. Therefore, the passing time can be considered as another identity of a vehicle. For a vehicle N_0, if we know its passing time at any location in a road network, we then obtain its trajectory.

From the travel times of individual vehicles, we are able to compute the total travel time between two locations, in particular between an O/D pair, as follows:

$$T([N_1,N_2];[x_1,x_2]) \quad = \quad \sum_{M=N_1}^{N_2} T(M;[x_1,x_2]), \tag{27}$$

where N_1 is the first vehicle and N_2 the last. We can see that, in Figure 2, the total travel time is equal to the area between the two N-curves. Then the average travel time for each vehicle will be

$$\bar{T}([N_1,N_2];[x_1,x_2]) \quad \equiv \quad \frac{T([N_1,N_2];[x_1,x_2])}{N_2-N_1} = \frac{\sum_{M=N_1}^{N_2} T(M;[x_1,x_2])}{N_2-N_1} \tag{28}$$

Moreover, for a road network, we can integrate travel times for all O/D pairs and, therefore, obtain the total travel time and the average travel time for the whole road network. These quantities are important indicators of the performance of a road network. Besides, we consider the loading time for an amount of flow to be released from an origin as another performance indicator.

Hence, the MCDKW simulation platform can be applied to evaluate traffic management and control strategies, such as route assignment and ramp metering algorithms.

4 Simulation results

In this section, we investigate the properties of the MCDKW model through simulations. We will show the evolution of traffic and examine the convergence of solutions. In this section, the diverge connecting links 2, 3, and 4 is modelled by Equation 11.

4.1 Simulation set-up

For these simulations, the network has the structure as shown in Figure 1. In this network, links 2, 3, and 5 have the same length, 20 miles, and the length of link 4 is 40 miles (not drawn to proportion); link 2 has three lanes, and the other links has two lanes; all links have the same triangular fundamental diagram (7):

$$Q(a,\rho) = \begin{cases} v_f \rho, & 0 \leq \rho \leq a\rho_c; \\ \frac{\rho_c}{\rho_j - \rho_c} v_f (a\rho_j - \rho), & a\rho_c < \rho \leq a\rho_j; \end{cases} \tag{29}$$

where ρ is the total density of all lanes, a the number of lanes, the jam density ρ_j=180 vpmpl, the critical density ρ_c=36 vpmpl, the free flow speed v_f=65 mph, the capacity of each lane $q_c = \rho_c v_f$=2340 vphpl, and the corresponding shock wave speed of jam traffic is $c_j = -\rho_c/(\rho_j - \rho_c) v_f \approx -17$ mph.

Initially, the road network is empty. Boundary conditions are defined as follows. Traffic supply at the destination is always $2q_c$. At origin, traffic demand at the origin is $3q_c$ during $[0, 6.0]$ and zero after that, and the proportion of commodity 0, which takes link 3 instead of 4, is always $\xi = 70\%$.

Links 2, 3, and 5 are partitioned into N cells each, and link 4 into $2N$ cells, with each cell of the same length, $\Delta x = 20/N$ miles. The total simulation time of 8.4 hours is divided into K time steps, with the length of a time step $\Delta t = 8.4/K$. In our simulations, we set $N/K = 1/30$. Thus the CFL (12) number is no larger than $v_f \Delta t/dx = 0.91$, which is valid for Godunov method (11).

4.2 Traffic patterns on the road network

We let $N = 400$ and $K = 12000$. Hence $\Delta x = 0.05$ miles=80 meters, and $\Delta t = 0.0007$ hours=2.52 seconds. Here the sizes of road cells and time steps are relatively small, in order for us to obtain results closer to those of the kinematic wave theories with the Godunov method.

The contour plots of the solutions are shown in Figure 3. From these figures, we can divide the evolution of traffic dynamics on the road network into three stages.

In the first stage starting from 0, vehicles embark link 2 with the free flow speed, prevail the link in its critical density $3\rho_c$, and arrive junction 1 at $t_1 = 20/65$ hr. At the diverge, junction 1, fluxes are computed from Equation 11: out-flux of link 2 is

$$f_{2,out} = \min\{3q_c, \frac{2q_c}{0.7}, \frac{2q_c}{0.3}\} = \frac{20}{7} q_c,$$

which is slightly smaller than the in-flux of link 2, in-flux of link 3 is $f_3 = 0.7 f_2 = 2q_c$, which is its capacity, and in-flux of link 4 is $f_4 = 0.3 f_2 = \frac{6}{7} q_c$, which is less than half of its capacity. After t_1, two streams of free flow form on links 3 and 4, and a backward travelling shock wave forms on Link 2, and the shock wave speed is

$$v_j = -\frac{1}{4} v_f.$$

At $t_2 = t_1 + 20/v_f$, the first vehicle on link 3 reaches junction 2, which is a merge. At t_2, the first vehicle on link 4 is half way back since the length of link 4 is double of link 3's. From the merge traffic flow model, Equation 7, we have the in-flux of link 5 as

$$f_{5,in} \quad = \quad \min\{2q_c, 2q_c\} = 2q_c,$$

which is also the out-flux of link 3. After t_2, the proportion of commodity 0 on link 5 is 1, as we can see on the bottom right figure.

The second stage starts at $t_3 = t_1 + 40/v_f = 60/65$ hr, when the first vehicle on link 4 reaches junction 2. After that, the in-flux of link 5 is still $2q_c$, but the proportion of commodity 0 reduces to 0.5714 since commodity 1 also contributes; on link 3, a new state forms at $\rho = 195.4290$ vpm, which is over-critical, and a shock wave travels upstream at the speed of $|c_j| \approx 17$ mph; on link 4, $\rho = 30.8571$ vpm, which is under-critical. At $t_4 = t_3 + 20/|c_j| = 140/65$ hr, the back-traveling shock on link 3 hits junction 1, and the traffic supply on link 3 is reduced. Therefore, the out-flux of link 2 is further reduced, and link 2 becomes more congested, as shown in the top left picture. This also reduces traffic flow on link 4, and the reduced flow reaches junction 2 at $t_5 = t_4 + 40/v_f = 180/65$ hr. After t_4, link 3 becomes less congested, and a rarefaction wave travels backward on it at $|c_j| \approx 17$ mph; the proportion of commodity on link 5 gets higher. From the bottom middle figure, we can see that at $t_5 = t_4 + 20/|v_j|$, traffic density on link 4 swings back a little due to the back traveling rarefaction on link 3. This shift is transported to junction 2 at $t_6 = t_5 + 40/v_f$ and oscillates traffic density on link 3 and the proportion of commodity 0 on link 5.

The third stage starts at $t_7 = 6$, when traffic demand from origin subsides to zero. After that, a shock forms on link 2 and travels forward, and propagates to link 4 and link 3. On link 4 the shock travels at v_f, and on link 3 it travels slower. This is why the proportion of commodity 0 on link 5 becomes 1 before it is emptied.

This simulation indicates that oscillation of traffic conditions can be caused by network merges and diverges even when the initial and boundary conditions are very nice. The traffic flow pattern on this road network suggests that, if we keep the same demand from the origin, an equilibrium state will be reached after some time.

The traffic patterns in Figure 3 can be partially observed from the top left figure in Figure 4, where the thicker four curves give cumulative flows for commodity 0, the thinner for commodity 1, and solid, dashed, dotted, and dash-dot curves are for cumulative flows at junction 0, 1, 2, and 3, respectively. In the bottom left figure, the solid lines are cumulative flows of commodity 0 at origin/destination, i.e., junction 0 and 3, the dashed curve is the number of commodity 0 vehicles in the network at a time, the dashed line shows the average number, the dotted curve is the travel time of a commodity 0 vehicle identified by its cumulative flow, and the dotted line is the average travel time. The bottom right figure has the same curves and lines as the bottom left figure, except that they are for commodity 1. Here travel time of individual vehicle is computed by Equation 26, total travel time by Equation 27, and average travel time by Equation 28. Although the formulas were developed for link travel times, it is valid for a network as long as vehicles of each commodity observe FIFO principle. Total (TTT) and average (ATT) travel times are listed in **Table** 1 (unit=hours).

Thus, vehicles that take link 4 on average use shorter time, which is still longer than the free flow travel time, 80/65 hr. Obviously, if all vehicles at origin decide to take link 3, the travel time, 60/65 will be the shortest possible travel time between the origin and destination. Therefore, this assignment fraction, 70%, is not an optimum one.

4.3 Convergence of the MCDKW simulation model

In this subsection, we study the convergence of the MCDKW simulation platform with increasing number of cells. Here we use the same road network, initial and boundary conditions as in the preceding subsection. Here we intend to show convergence in average travel times of both commodities.

Denoting the average travel time of a commodity, T, as a function of the number of cells, N; i.e., $T = T(N)$, we can define the relative error, from N to $2N$, by

$$\epsilon^{2N-N} = |T(2N) - T(N)|. \tag{30}$$

Then a convergence rate is computed by

$$r = \log_2(\frac{\epsilon^{2N-N}}{\epsilon^{4N-2N}}). \tag{31}$$

The convergence rates of the average travel times are given in **Table** 2.

From the table, we can see that average travel times are also convergent in first order. Note that this convergence is different from the aforementioned traffic conditions converging to certain equilibrium state. Moreover, we can see that the results with $N = 200$ is already accurate enough in this case. Since the computation time of the MCDKW simulation platform is quadrupled when N is doubled, in later simulations, we use $\Delta x = 0.1$ mile=160 meters and $\Delta t = 0.0014$ hours= 5.04 seconds with the same simulation period.

5 Discussions

In this paper, we proposed the Multi-Commodity Discrete Kinematic Wave (MCDKW) model. In this model, we integrated various kinematic wave theories for individual components and carefully discussed commodity-based kinematic wave theories. We further demonstrated how to obtain cumulative flows and travel times from outputs of MCDKW simulations. Simulations show that numerical results converge to FIFO solutions although the FIFO condition is not strictly enforced in the discrete form of commodity-based kinematic wave theories.

Different from many existing simulation packages, where traffic is tracked down to the vehicle level, the MCDKW simulation concerns traffic conditions down to the commodity level. The simulation model is designed for handling very large road networks and can be applied in dynamic traffic assignment, dynamic O/D estimation, and so forth. However, as pointed out earlier, the effects of "departure from FIFO" should be carefully considered in these applications.

In the future, the MCDKW model can be enhanced in three aspects. Theoretically, vehicle types and special lanes can be incorporated (18), and nonequilibrium continuum models (19) may also be integrated. Numerically, parallel algorithms can be applied to improve computational speed since traffic conditions on different links can be updated simultaneously, and the consumption of computer memory will be checked. Finally, for different applications, we also plan to design different input/out interfaces. For example, the network structure can be imported from GIS (Geographic Information System) data files, and boundary conditions and output can be manipulated for different applications.

Acknowledgement

This research was partially funded by the National Science Foundation under Grant Number 9984239 and by the University of California Transportation Center. The views are those of the authors alone.

References

[1] Carlos F. Daganzo. The cell transmission model II: Network traffic. *Transportation Research B*, 29(2):79–93, 1995.

[2] J. P. Lebacque. The godunov scheme and what it means for first order traffic flow models. In *The International Symposium on Transportation and Traffic Theory*, Lyon, France, 1996.

[3] R. Vaughan, V. F. Hurdle, and E. Hauer. A traffic flow model with time dependent o-d patterns. In *Ninth International Symposium on Transportation and Traffic Theory*, pages 155–178. VNU Science Press, 1984.

[4] R. Jayakrishnan. *In-vehicle information systems for network traffic control: a simulation framework to study alternative guidance strategies*. PhD thesis, The University of Texas at Austin, 1991.

[5] Carlos F. Daganzo. The cell transmission model: a dynamic representation of highway traffic consistent with hydrodynamic theory. *Transportation Research B*, 28(4):269–287, 1994.

[6] J. D. Lenonard II. A tool for evaluating freeway congestion. Technical report, Georgia Institute of Technology, http://traffic.ce.gatech.edu/gtwaves, 1998.

[7] G. F. Newell. A simplified theory of kinematic waves in highway traffic I: General theory. II: Queuing at freeway bottlenecks. III: Multi-destination flows. *Transportation Research B*, 27:281–313, 1993.

[8] C. Buisson, J. P. Lebacque, and J. B. Lesort. STRADA, a discretized macroscopic model of vehicular traffic flow in complex networks based on the godunov scheme. In *CESA'96 IMACS Multiconference*, Lille, France, July 9-12 1996.

[9] C. Buisson, J. P. Lebacque, J. B. Lesort, and H. Mongeot. The STRADA model for dynamic assignment. In *3rd World Congress on Intelligent Transport Systems*, Orlando, Florida, 1996.

[10] Carlos F. Daganzo. The lagged cell-transmission model. In *The 14th International Symposium on Transportation and Traffic Theory*, Jerusalem, Israel, 1999.

[11] S. K. Godunov. A difference method for numerical calculations of discontinuous solutions of the equations of hydrodynamics. *Matematicheskii Sbornik*, 47:271–306, 1959. In Russian.

[12] R. Courant, K. Friedrichs, and H. Lewy. ber die partiellen differenzengleichungen der mathematischen physik. *Mathematische Annalen*, 100:32–74, 1928.

[13] W. L. Jin and H. M. Zhang. The inhomogeneous kinematic wave traffic flow model as a resonant nonlinear system. *Transportation Science*, 37(3): 294–311, August 2003.

[14] W. L. Jin and H. Michael Zhang. On the distribution schemes for determining flows through a merge. *Transportation Research B*, 37(6):521–540, July 2003.

[15] W. L. Jin and H. Michael Zhang. An instantaneous kinematic wave theory of diverging trac. 2002. Submitted.

[16] M. Papageorgiou. Dynamic modelling, assignment and route guidance in traffic networks. *Transportation Research B*, 24(6):471–495, 1990.

[17] W. L. Jin and H. M. Zhang. A kinematic wave traffic flow model for diverges, part ii: The coupled version. 2001. working paper.

[18] Carlos F. Daganzo. A behavioral theory of multi-lane traffic flow. part I: Long homogeneous freeway sections. II: Merges and the onset of congestion. *Transportation Research B*, 36:131–169, 2002.

[19] W. L. Jin and H. Michael Zhang. Studies on a nonequilibrium continuum traffic flow model with frozen "sound wave" speed. January 2003. Presented at TRB 2003 Annual Meeting.

List of Tables

List of Figures

	Total Number of Vehicles	TTT	ATT
Commodity 0	23,859	4.7291×10^4	1.9822
Commodity 1	10,225	1.7372×10^4	1.6989

Table 1: Total travel time (TTT) and average travel time (ATT) for two commodities

Commodity 0	N=200	N=400	N=800	N=1600	N=3200
ATT	1.98189893	1.98215215	1.98227240	1.98234941	1.98239377
Error $[10^{-3}]$		0.2532	0.1202	0.07700	0.0444
Rate			**1.074**	**0.6430**	**0.7958**
Commodity 1	N=200	N=400	N=800	N=1600	3200
ATT	1.69922958	1.69892887	1.69877593	1.69871236	1.69868722
Error $[10^{-3}]$		-0.3007	-0.1529	-0.0636	-0.0251
Rate			**0.9755**	**1.2664**	**1.3384**

Table 2: Convergence rates for the MCKW simulation platform

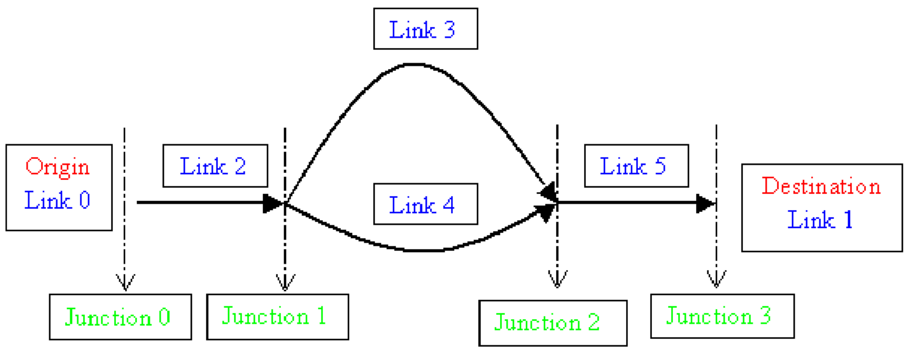

Figure 1: A demonstration road network

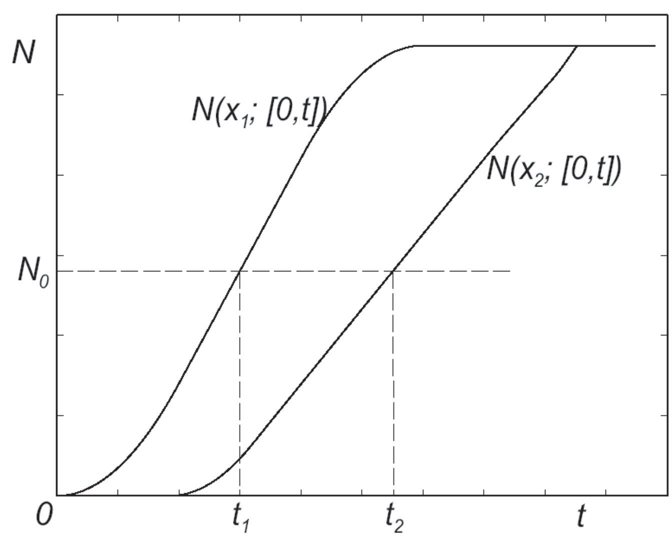

Figure 2: Cumulative flows and travel time

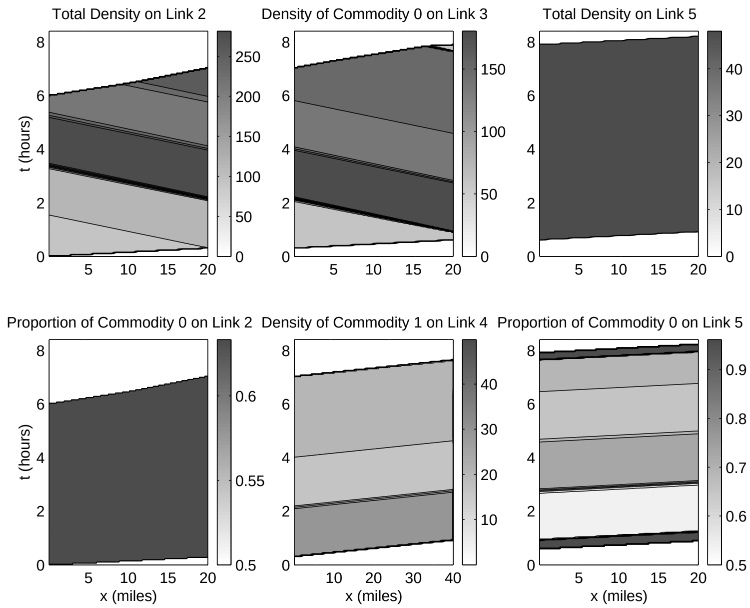

Figure 3: Contour plots of network traffic flow

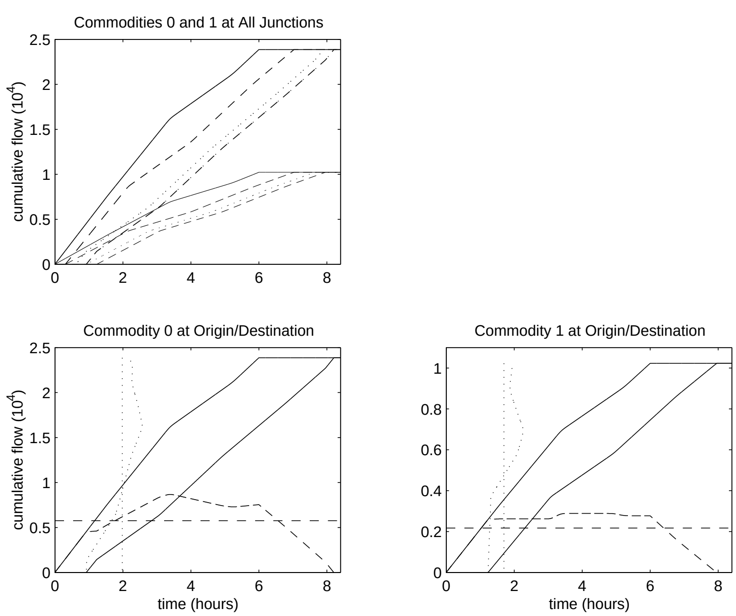

Figure 4: N-curves and travel times of each commodity in the road network